EUROPEAN ORGANIZATION FOR NUCLEAR RESEARCH

KK/gm

CERN/PS 86-12 (EA)
2.6.1986

A NEW TYPE OF BEAM PROFILE MONITOR

V. Agoritsas*, C. Nemoz+, K. Kuroda+ and D. Sillou+

A B S T R A C T

A new type of position sensitive monitor is under development in order to meet the demands of beam controls in the field of modern accelerators. Tests on the first prototype revealed the possibility of realizing a simple and reliable profile monitor for a wide range of beam energy and intensity.

* CERN, Geneva, Switzerland
+ LAPP, Annecy-le-Vieux, France

Submitted for publication to Nuclear Instruments and Methods

1. INTRODUCTION

Progress in particle detectors based on the secondary emission phenomenon has been made so far in parallel to the development of modern particle accelerators. High-energy proton and antiproton beams of the CERN Proton Synchrotron Complex are in fact basically monitored by a number of different types of detectors based on this phenomenon. For example, the secondary emission chamber for measurements of the intensity of both the fast and slow extracted beams was in operation as early as the middle of 1960s[1,2]. Affording high gain and position sensitivity to such a type of detectors it now becomes possible to conceive a new type of beam monitor.

In 1978 a new kind of dynode has been proposed on the basis of a scaling property of secondary electron trajectories inside the electric and magnetic fields[3]. Since that time this kind of dynode has been extensively applied not only to position sensitive photomultipliers[4,5], but also to other modern photomultipliers[6], profiting from several merits of the scaling property, namely, localization of secondary electrons, immunity to magnetic fields, high linearity of gain and fast time response.

As a natural extension of such a high performing dynode system and to meet the demands of beam controls in the field of modern accelerators, we have constructed in collaboration with Hamamatsu Photonics a beam monitor for the purpose of measuring the image of beam spots, in particular at very low energies, in a wide range of beam intensity.

Compared to other types of detectors currently used in the field of particle physics, such as proportional chamber, solid-state detector etc. our device could be characterized by its carefree nature thanks to components made entirely of stable inorganic materials almost free from any destructive aging effects and resistant to the radiation.

In this paper we report on the first results confirming the feasibility of such a type of position-sensitive beam monitor, while a number of improvements are still under way in our laboratories.

2. Experimental Set-up

Figure 1 shows schematically the structure of the present prototype. The essential part consists of 13 stages of grid type dynodes 100 mm in useful diameter. Each stage has two layers of grid made of CuBe ~ 60 μm in average thickness. A thin aluminum foil, 50 μm thick, placed in front of the first dynode releases secondary electrons when traversed by charged particles or converted γ-rays. After multiplication of electrons by the dynode system, the flux of secondary electrons falls onto an array of 20 anode strips 3 mm wide aligned in one direction with a gap of 1 mm.

The whole system is placed inside a stainless steel vacuum-tight vessel with INOX foil windows 35 μm thick. The vessel was permanently pumped by an ion pump of 8 L/sec which kept a vacuum pressure lower than 10^{-8} mm Hg.

In order to improve the localization of secondary electrons during the multiplication process an axial magnetic field variable from 0 to 400 G can be applied by a couple of Helmholtz coils.

All the adjacent anode strips were connected in series through coaxial cables of 3-5 ns in order to reconstruct the position of incident particles by a time-centroid method described elsewhere[7].

3. Results

A series of measurements has been done using different kinds of radiation sources.

In order to estimate the spread of secondary electrons at the level of anode strips we first measured the coincidence counting rates between the adjacent strips, which say how many strips are excited simultaneously by a single event. Figure 2 shows the results obtained by a collimated γ-source (Cs^{137}). For different values of the axial magnetic field the threshold on the anode signals was adjusted so that the single counting rate remains almost constant. Without magnetic field the level of 10 % correlation, for example, extends over 7 strips, i.e. a distance of 28 mm. By increasing the magnetic field the spread retracts quickly to attain only two strips at the

maximum strength of the magnetic field, ~ 400 G. This is in good agreement with the intrinsic resolution, 5-6 mm, usually observed in a position-sensitive photomultiplier with the same type of dynode structure[4].

Spatial distribution of events was obtained by a pulse-height analyser after conversion of the time lag between the anode signals arriving to the right and the left boundaries of the delay line. A typical example of the distributions obtained with a collimated 200 MeV/c π^- beam is shown in Fig. 3a. In spite of significant backgrounds, which will be discussed later, one can see clearly a pronounced peak sitting on a smooth background (Fig. 3b). The peak follows well the position of the beam as shown in Fig. 4, where the beam was moved by a step of 10 mm. The linearity between the peak position and the real coordinate is plotted in Fig. 5. Data presented by solid circles come from similar measurements done with collimated γ-rays. In both cases the linearity is quite good in almost the full range of the sensitive area (80 x 80 mm^2).

A rough estimate of the spatial resolution can be given by a couple of the peaks obtained at a known distance. The resolution varies slightly as a function of the magnetic field.

Figure 6 shows an example obtained for 100 G and a distance of 30 mm between the peaks. The FWHM of the peaks is about 5 mm. Subtracting the geometrical size of the collimated beam, ~ 3 mm at the level of the aluminum foil, the final resolution of the device is about 4 mm in FWHM.

It is worthwhile to mention that the resolution without magnetic field is kept in a range of 5-6 mm and does not decrease drastically as one would expect from the spread of secondary electrons (see Fig. 2).

The detection efficiency of the device has also been measured by putting the device in coincidence with two scintillation counters placed upstream and downstream. For a suitable threshold on the anode signals the efficiency was found to be about 5 % for 200 MeV/c π^-.

4. Discussions

The first remark concerns the nature of backgrounds: As shown in Figs. 3a to 3d two kinds of backgrounds can be treated separately: the first one is a proper noise of the device coming mainly from the cold emission of electrons and the ionization of residual gases, producing therefore a fairly flat distribution over the full sensitive area (Fig. 3b). The counting rate of this kind of background was about 15/sec at the normal working conditions. The second one is a background associated to the incident radiation. After subtracting the proper noise the event distribution (Fig. 3c) can be well fitted, as shown in Fig. 3d, by a sum of two components; narrow Gaussian-like distribution and wide 3rd-order polynomial.

The ratio, R = 1st component/2nd one, was about 1.2 for this example of the event distributions. The first component can be interpreted as a contribution of the normal events detected due to the secondary electron(s) produced at the level of the aluminum foil.

On the other hand, the nature of the second component is not clearly identified at the present time. However, we can mention here some hypothesis on the possible sources; (a) external source such as an halo around the collimated beam by slit, involving not only charged particles but any kind of radiation such as γ-rays, and/or (b) internal source such as soft γ or X-rays internally created on the materials along the trajectory of the incident particles.

In order to obtain more information some additional measurements have been done; by selecting the events with the aid of two scintillation counters placed upstream and downstream the distribution becomes very Gaussian-like as shown in Figs. 7a to 7d, giving the ratio $R \simeq 5.8$. From this result, although the second hypothesis cannot be completely removed if the internal creation could take place only by totally absorbed incident radiation, the first hypothesis seems to be more plausible. This argument is also supported by another measurement done with a strongly focused antiproton beam from LEAR, which gave $R \simeq 2.3$.

Anyway, a straightforward check on the nature of this kind of background has to be done by taking into account the fact that our device is sensitive not only to charged particles but also to γ-rays which can be converted on the materials situated at the first multiplication stages.

Let us now argue some possible improvements in the near future. The result obtained without magnetic field suggests a possibility of eliminating the axial magnetic field without spoiling too much the spatial resolution. As already demonstrated in the field of the position-sensitive photomultipliers, it is possible to limit the spread of secondary electrons to a reasonable width, without magnetic field, only by reducing the interdynode distance[8]. Furthermore, following the scaling property of electron trajectories[4] a reduction of all the dynode dimensions, including those of grid bars, will improve automatically the localization of electrons. For example, a dynode structure consisting of fine grids of 0.1 mm in lateral size of the bars, instead of 0.5 mm actually adopted, will give a final spatial resolution much better than 1 mm even without the axial magnetic field.

5. Conclusion

A new type of position-sensitive monitor, based on the secondary emission, has been tested using different kinds of radiation sources. The spatial resolution was found to be ~ 4 mm in FWHM with a weak axial magnetic field of ~ 100 G.

Although a more detailed study on the nature of certain background remains to be done, one can already confirm the feasibility of such a type of beam monitor having inherently the following advantages:

- it is almost free from any aging effects due to radiation damages;
- it works inside high vacuum without window materials, and is able to detect very low-energy charged particles, and
- high proper gain of the dynode system, ~ 10^7, which is of course insensitive to electromagnetic parasites, assures a good stability of its operation under hot environments.

In addition, the possibility of eliminating the axial magnetic field will lead us to realize a compact and reliable profile monitor for a wide range of beam energy and intensity.

Acknowledgements

We are much indebted to Hamamatsu Photonics who have willingly realized the dynode system following our specifications. We express our gratitude in particular to Mr. H. Kume for his efficient help during the preparation.

We thank Dr. D.J. Simon for his constant interest and advice which enabled us to carry out this work under the best conditions.

It is a pleasure to express our thanks also to Messrs. J. Haffner, J.P. Bovigny, M. Berthet, J. Ditta and L. Giacobone for their efficient technical assistance.

References

1. V. Agoritsas and J.J. Merminod, CERN/MPS/10-71-9.

2. V. Agoritsas and C.D. Johnson, CERN/MPS/10/NOTE 71-51.

3. K. Kuroda, D. Sillou and F. Takeutchi, French Patent N° 7836148 applied by ANVAR-France (Dec. 22, 1978), and US Patent N° 4339684 (July 13, 1982).

4. K. Kuroda, D. Sillou and F. Takeutchi, Rev.Sci.Instr. 52 (1981) 337.

5. H. Kume, S. Suzuki, J. Tanaka and K. Oba, IEEE Trans.Nuc.Sci. NS-32(1) (1985) 448.

6. S. Orito, T. Kobayashi, K. Suzuki, M. Ito and A. Sawaki, Nuc.Instr. and Meth. 216 (1983) 439.

7. J. Ditta, K. Kuroda, C. Nemoz and D. Sillou, to be published in Nuc.Instr. and Meth.

8. K. Kuroda, French Patent N° 8407142 (May 9, 1984) applied by ANVAR-France. See also Ref. 5 as an example of the experimental confirmations.

Figure Captions

Fig. 1 Experimental set-up.

Fig. 2 Number of correlated anode strips at different strenghts of the axial magnetic field.

Fig. 3 Typical example of event distribution obtained with a collimated π^- beam of 200 MeV/c.

a) original distribution

b) proper noise of the apparatus

c) fit by two components after subtraction of the noise

d) corresponding fit functions.

Fig. 4 Event distributions for different beam positions.

Fig. 5 Linearity of the reconstructed position as a function of the real coordinate X(cm).

Δ - data from 200 MeV/c π^- beam.

● - data from collimated γ-rays.

Fig. 6 Event distribution obtained by moving π^- beam by a distance of 30 mm.

Fig. 7 Distribution of collimated π^- after selection of events by two scintillation counters.

a) to d); see Fig. 3 for corresponding items.

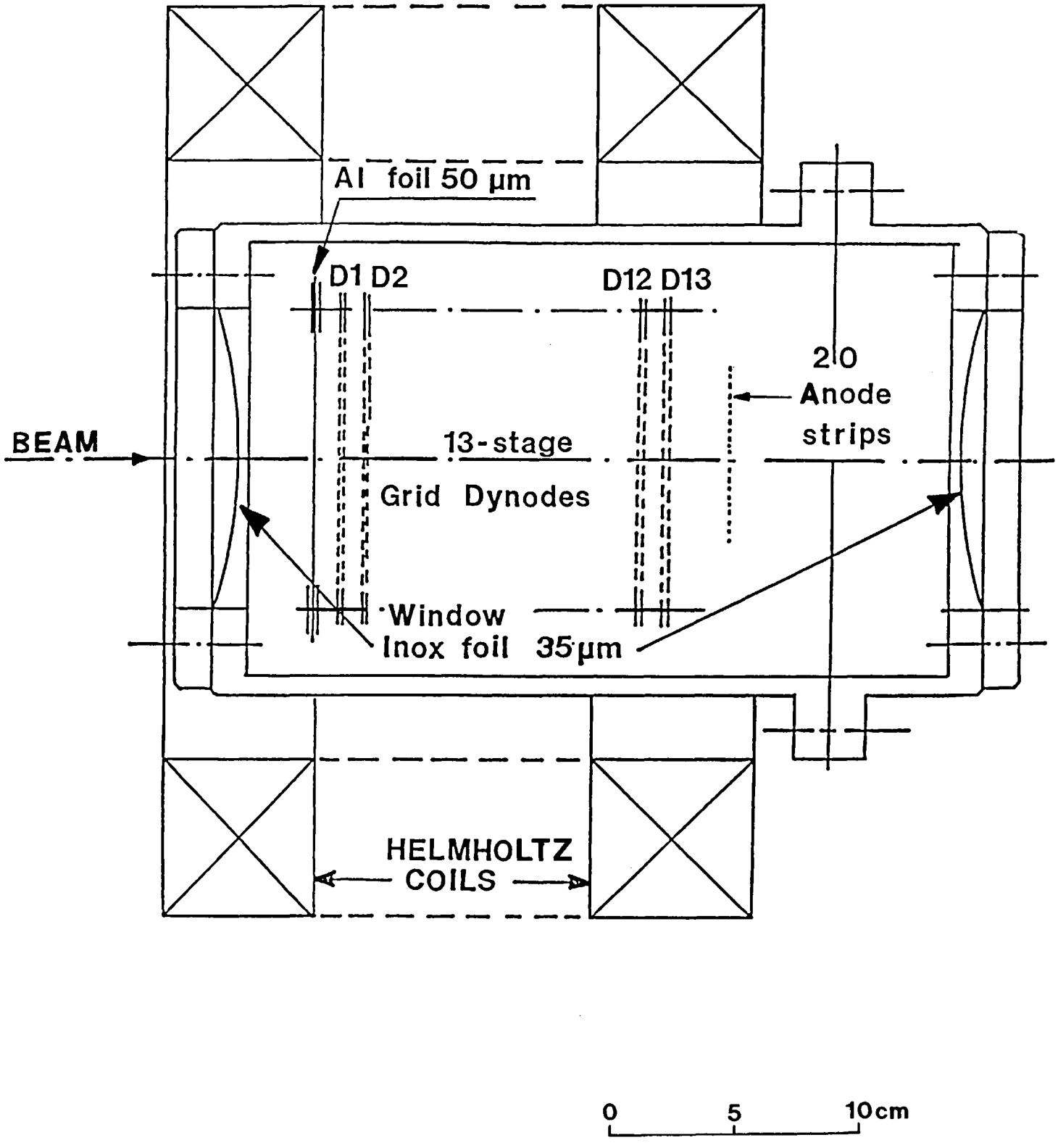
Al foil 50 µm
D1 D2
D12 D13
210
Anode
strips
BEAM
13-stage
Grid Dynodes
Window
Inox foil 35µm
HELMHOLTZ
COILS
0
5
10cm

Fig. 1

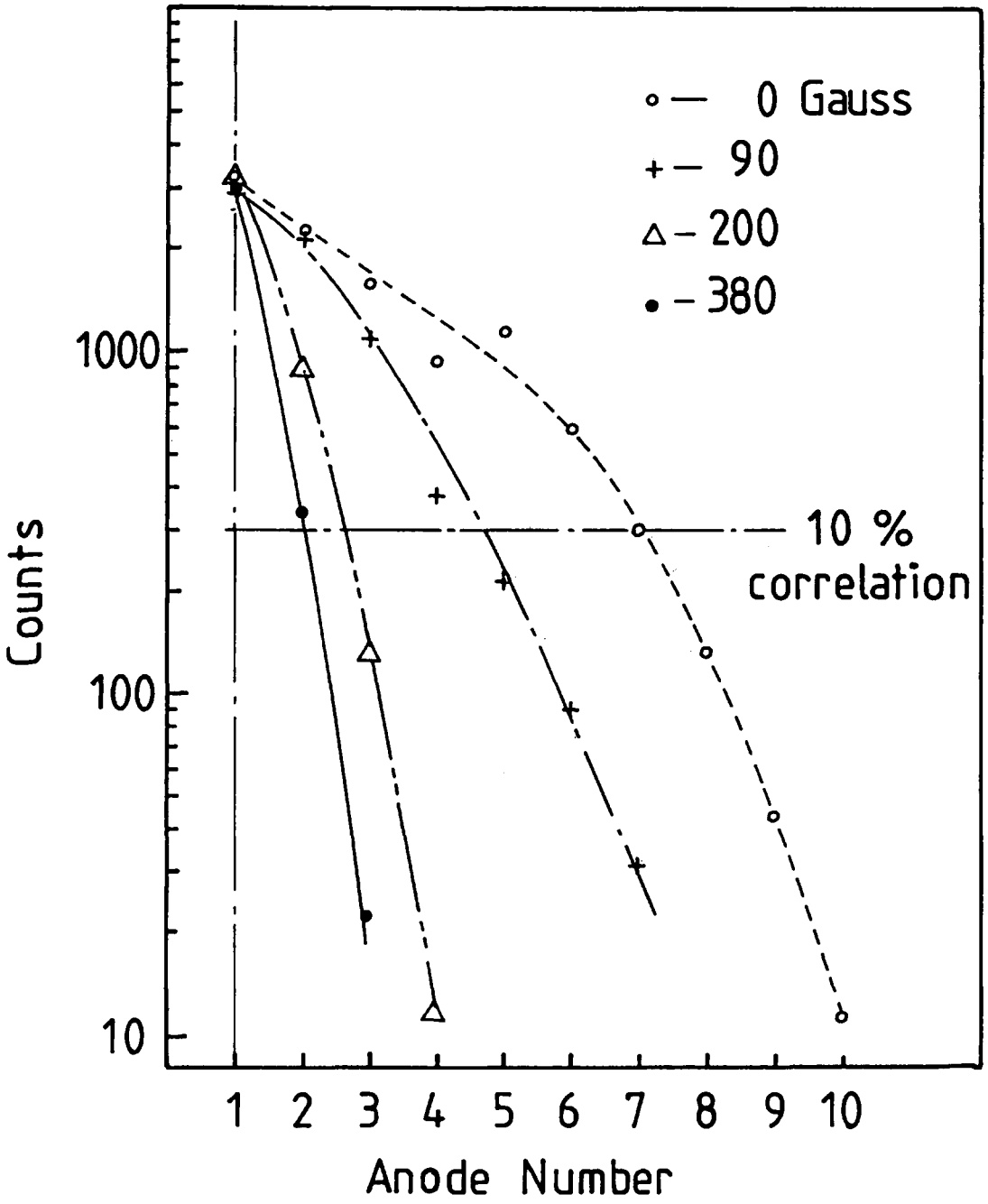
o — 0 Gauss
+ — 90
△ – 200
• – 380
1000
100
10
Counts
10 %
correlation
1 2 3 4 5 6 7 8 9 10
Anode Number

Fig. 2

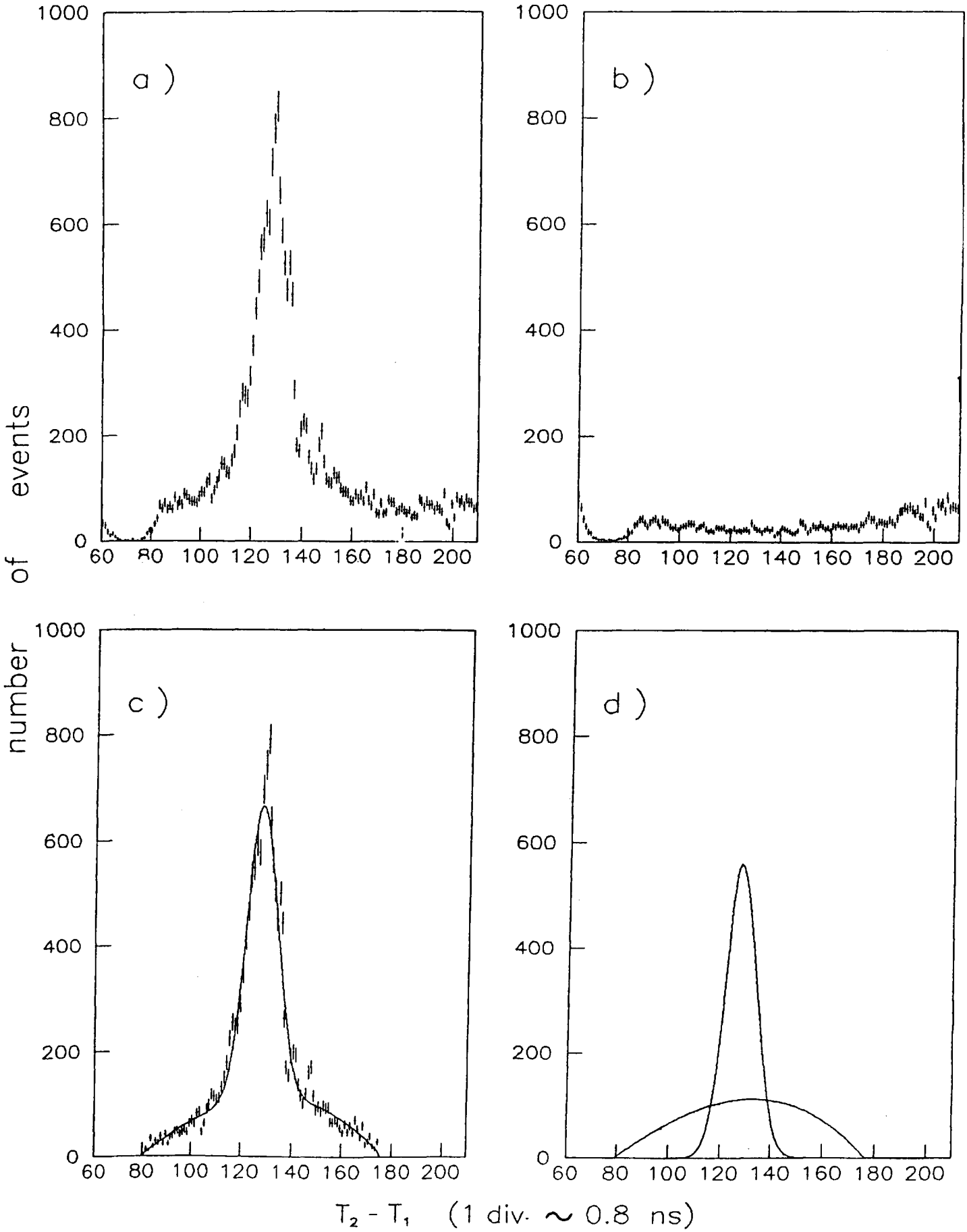
a)
b)
c)
d)
1000
800
600
400
200
0
60 80 100 120 140 160 180 200
number of events
$T_2 - T_1$ (1 div. ~ 0.8 ns)

Fig. 3

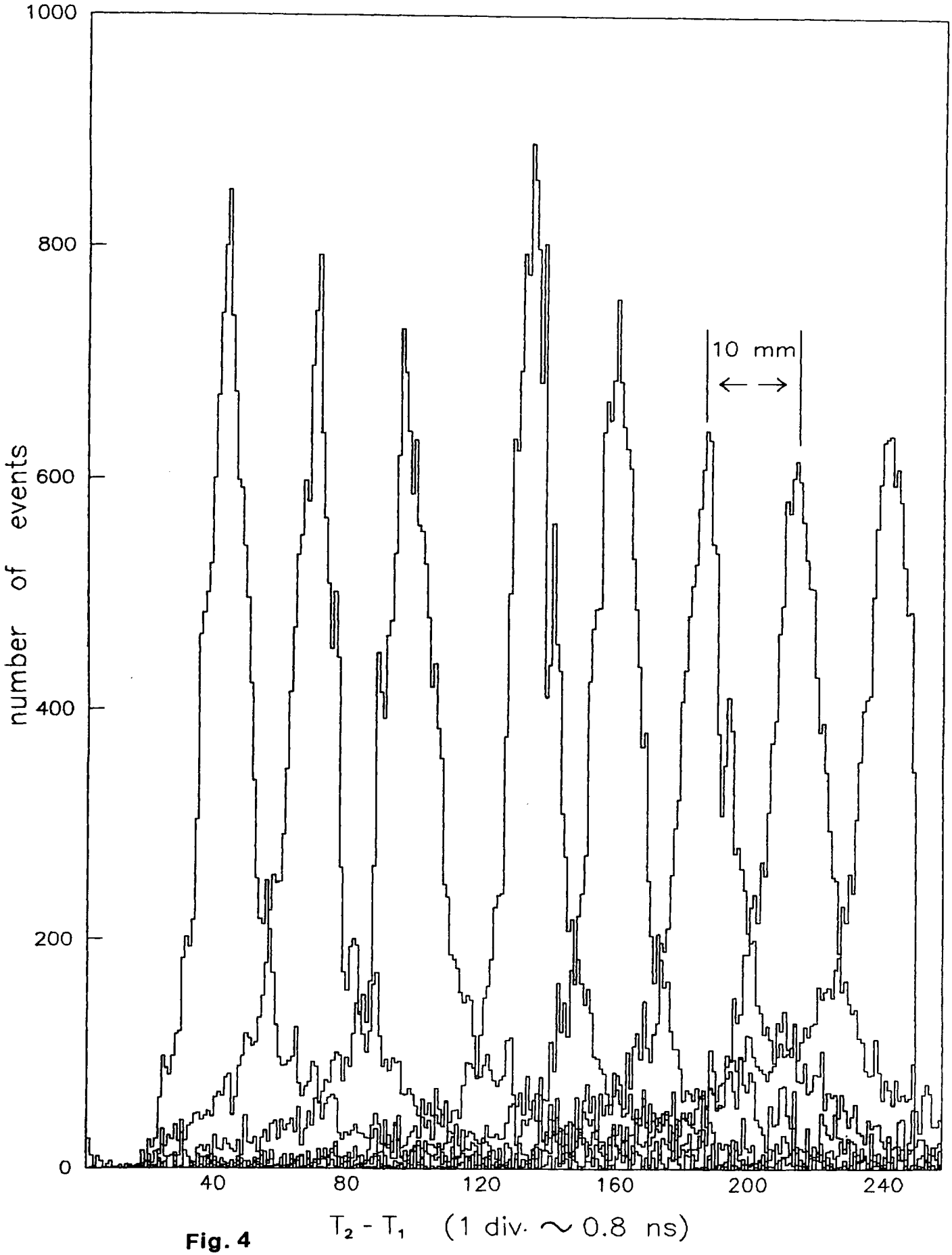
1000
800
600
400
200
0
number of events
10 mm
40
80
120
160
200
240
T₂ - T₁ (1 div. ~ 0.8 ns)

Fig. 4

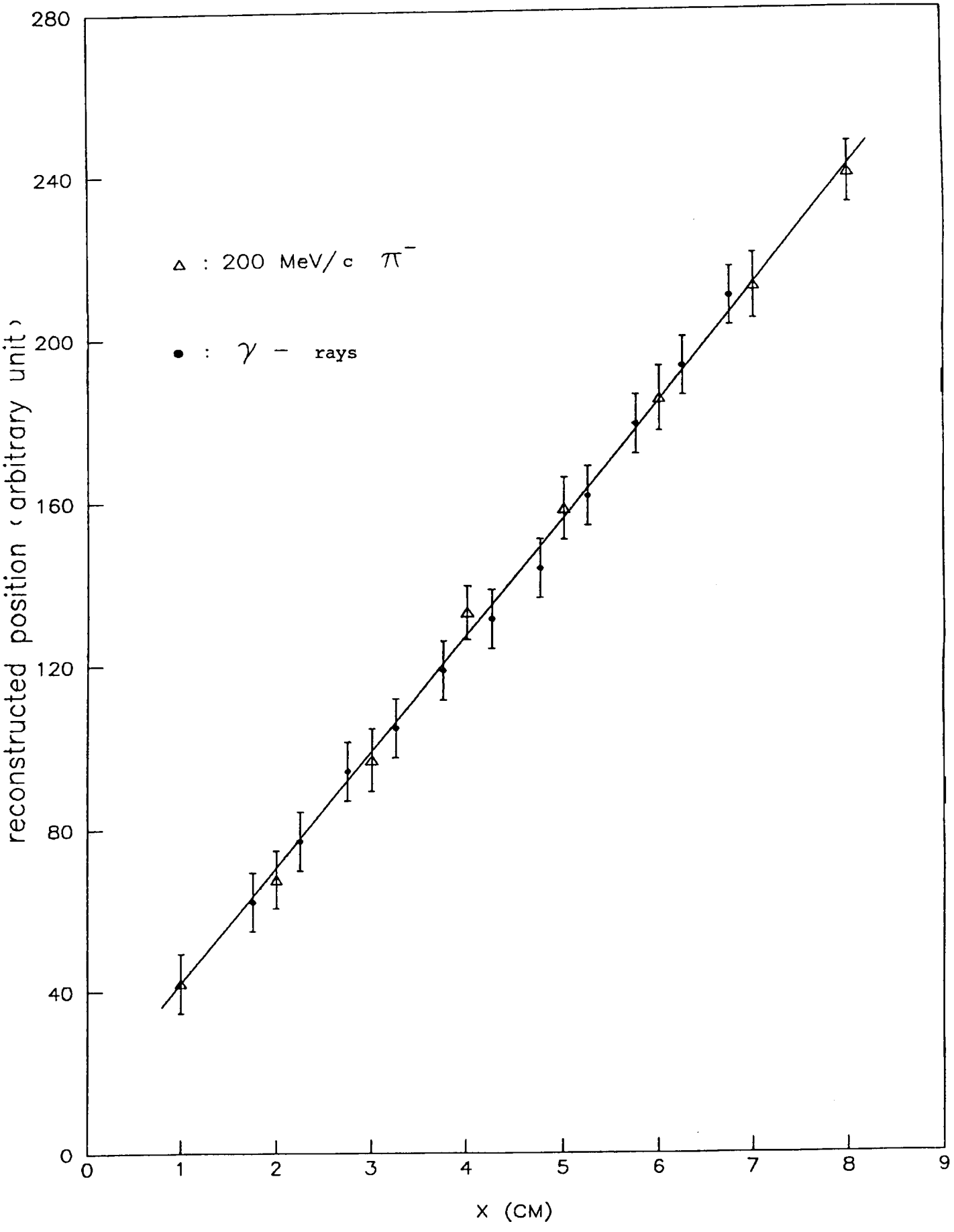
280
240
200
160
120
80
40
0
reconstructed position (arbitrary unit)
△ : 200 MeV/c π⁻
● : γ - rays
0
1
2
3
4
5
6
7
8
9
X (CM)

Fig. 5